Systems Analysis of Guard Cell Membrane Transport for Enhanced Stomatal Dynamics and Water Use Efficiency[1][W][OPEN]

Yizhou Wang, Adrian Hills, and Michael R. Blatt*

Laboratory of Plant Physiology and Biophysics, Institute of Molecular, Cell and Systems Biology, University of Glasgow, Glasgow G12 8QQ, United Kingdom

Stomatal transpiration is at the center of a crisis in water availability and crop production that is expected to unfold over the next 20 to 30 years. Global water usage has increased 6-fold in the past 100 years, twice as fast as the human population, and is expected to double again before 2030, driven mainly by irrigation and agriculture. Guard cell membrane transport is integral to controlling stomatal aperture and offers important targets for genetic manipulation to improve crop performance. However, its complexity presents a formidable barrier to exploring such possibilities. With few exceptions, mutations that increase water use efficiency commonly have been found to do so with substantial costs to the rate of carbon assimilation, reflecting the trade-off in CO_2 availability with suppressed stomatal transpiration. One approach yet to be explored in detail relies on quantitative systems analysis of the guard cell. Our deep knowledge of transport and homeostasis in these cells gives real substance to the prospect for reverse engineering of stomatal responses, using in silico design in directing genetic manipulation for improved water use and crop yields. Here we address this problem with a focus on stomatal kinetics, taking advantage of the OnGuard software and models of the stomatal guard cell recently developed for exploring stomatal physiology. Our analysis suggests that manipulations of single transporter populations are likely to have unforeseen consequences. Channel gating, especially of the dominant K^+ channels, appears the most favorable target for experimental manipulation.

Stomata are pores that provide the major route for gaseous exchange across the impermeable cuticle of leaves and stems (Hetherington and Woodward, 2003). They open and close in response to exogenous and endogenous signals and thereby control the exchange of gases, most importantly water vapor and CO_2, between the interior of the leaf and the atmosphere. Stomata exert major controls on the water and carbon cycles of the world (Schimel et al., 2001) and can limit photosynthetic rates by 50% or more when demand exceeds water supply (Ni and Pallardy, 1992). Stomatal transpiration is at the center of a crisis in water availability and crop production that is expected to unfold over the next 20 to 30 years; indeed, global water usage has increased 6-fold in the past 100 years, twice as fast as the human population, and is expected to double again before 2030, driven mainly by irrigation and agriculture (United Nations Educational, Scientific and Cultural Organization, 2009).

Guard cell transport is integral to controlling stomatal aperture. Guard cells surround the stomatal pore and respond in a well-defined manner to an array of extracellular signals, including light, to regulate its aperture. Guard cells coordinate membrane transport within a complex network of intracellular signals (Willmer and Fricker, 1996; Blatt, 2000a, 2000b; Hetherington and Woodward, 2003; Shimazaki et al., 2007) to regulate fluxes, mainly of K^+, Cl^-, and malate, driving cell turgor and stomatal aperture. Our deep knowledge of these processes has made the guard cell the best known of plant cell models for membrane transport, signaling, and homeostasis (Willmer and Fricker, 1996; Blatt, 2000b; Roelfsema and Hedrich, 2010; Hills et al., 2012). This knowledge gives real substance to the prospect for reverse engineering of stomatal responses, using in silico design in directing genetic manipulation for improved crop yields, especially under water-limited conditions.

Water use efficiency (WUE; defined as the amount of dry matter produced per unit of water transpired) is directly related to stomatal function. Thus, at the practical level, stomata represent an important target for breeders interested in manipulating crop performance. A large body of data relates stomata, transpiration, and carbon assimilation (Willmer and Fricker, 1996; Farquhar et al., 2001; Hetherington and Woodward, 2003; Lawson et al., 2011). Several examples illustrate how manipulating of stomatal characteristics can affect WUE (Fischer et al., 1998; Rebetzke et al., 2002; Masle et al., 2005; Eisenach et al., 2012). With few exceptions,

[1] This work was supported by the Biotechnology and Biological Sciences Research Council (grant nos. BB/H024867/1, BB/F001630/1, BB/L001276/1, and BB/H009817/1 to M.R.B.).

* Address correspondence to michael.blatt@glasgow.ac.uk.

The author responsible for distribution of materials integral to the findings presented in this article in accordance with the policy described in the Instructions for Authors (www.plantphysiol.org) is: Michael R. Blatt (michael.blatt@glasgow.ac.uk).

[W] The online version of this article contains Web-only data.

[OPEN] Articles can be viewed online without a subscription.

www.plantphysiol.org/cgi/doi/10.1104/pp.113.233403

however, mutations that increase WUE commonly do so at the expense of carbon assimilation, reflecting the trade-off in CO_2 availability with suppressed stomatal transpiration.

Stomatal movements generally lag behind short-term changes in available light associated with sunflecks and shadeflecks (Pearcy, 1990; Lawson et al., 2012; Lawson and Blatt, 2014). This hysteresis in response, between stomatal aperture and gas exchange on one hand and photosynthetic capacity on the other, can lead alternately to periods of assimilation limited by stomatal conductance, and of high transpiration without corresponding rates of assimilation (Lawson et al., 2011). It has been argued that such hysteresis in stomatal responsiveness with the demand for CO_2 erodes assimilation and WUE, with substantial consequences for long-term yield (Vico et al., 2011; Eisenach et al., 2012; Lawson et al., 2012; Lawson and Blatt, 2014). If so, then improving WUE with gains in assimilation should be possible if the speed of stomatal responsiveness can be enhanced. However, the complexity of guard cell transport presents a formidable barrier to exploring such possibilities. Here we address this problem, taking advantage of OnGuard models of the stomatal guard cell. We explore in silico the potential for enhancing stomatal kinetics through single transporter (single gene product) manipulations. Our results identify the gating of the dominant K^+ channels as the most promising target for experimental manipulation.

RESULTS AND DISCUSSION

We previously developed the OnGuard software for quantitative dynamic systems modeling of the guard cell (Chen et al., 2012; Hills et al., 2012). OnGuard models incorporate explicitly all of the wealth of molecular, biophysical, and kinetic knowledge for guard cell transport, osmolyte metabolism, and H^+ and Ca^{2+} buffering, and they couple this knowledge to guard cell volume, turgor, and stomatal aperture. OnGuard applications have yielded an abundance of counterintuitive, emergent characteristics in the function of wild-type guard cells of the crop *Vicia* and the model plant Arabidopsis (*Arabidopsis thaliana*; Chen et al., 2012; Wang et al., 2012). Applied to the Arabidopsis *slac1* anion channel and *ost2* ATPase mutants, the latter has also demonstrated new and unexpected connections between membrane transport, metabolism, and stomatal dynamics, uncovering a previously unrecognized homeostatic network that was subsequently verified experimentally (Wang et al., 2012; Blatt et al., 2013). Thus, OnGuard models incorporate the predictive power needed to guide reverse engineering of stomatal function starting with molecular manipulations in silico.

We carried out an analysis of stomatal opening and closing, using OnGuard to predict the consequences of targeted genetic manipulations. At present, OnGuard reflects the characteristics of stomata in isolation (Hills et al., 2012) and does not incorporate feedback from the transpiration stream nor from internal pCO_2 in the leaf. As a consequence, kinetic relaxations of OnGuard models are prolonged, especially during opening, but are nonetheless scaled appropriately. The simulations presented here were designed to test the sensitivity to changes over a narrow range of parameters potentially tractable through genetic manipulation for each of the major transporters. We compared these outputs with similar analyses carried out for the wild-type (control) parameter set. For simplicity, each of the transporters was tested with population densities adjusted by factors of 0.5- and 2-fold. We followed a similar approach in varying the macroscopic gating characteristics of several voltage-sensitive ion channels. Outputs were quantified on the basis of the maximum rates of stomatal opening and closing, and on the dynamic range of apertures. Simulations used a standard diurnal cycle with a saw-tooth rise and fall in light over 12 h followed by 12 h of dark; as before, light was used as the driver for Suc and malate synthesis, and for the primary ATPase activities at the two membranes (Chen et al., 2012) employing, as a starting point, the Arabidopsis and *Vicia* models previously described (Hills et al., 2012; Wang et al., 2012). Analysis of the two models yielded similar results when scaled to the guard cell dimensions. To avoid duplication, only the results for the Arabidopsis model are reported here.

Manipulating Transporter Populations

These manipulations are comparable with variations in the steady-state levels of transporter expression such as might be achieved through moderated overexpression and RNA interference-mediated suppression. Figure 1A shows the simulation outputs for the wild type (control) and for 0.5x Kout and SLAC, equivalent to suppressing the population of outward-rectifying K^+ channels (Hosy et al., 2003) and SLAC1 anion channels (Negi et al., 2008; Wang et al., 2012) in the guard cell to 50% of the wild type. The daylight period is marked by stomatal opening that progresses over the first 6 to 8 h and, as the light decayed to near its midpoint ($K_{1/2}$) for activation of malate synthesis and the ATPases at its end, by stomatal closing (Chen et al., 2012; Wang et al., 2012). The Figure 1A inset also provides the outputs used for comparisons. Reducing the K^+ and anion channel populations had visible effects on the dynamic range of stomatal movements. It also had substantial, although less obvious, effects on stomatal kinetics. These characteristics are summarized in Figure 1, B and C, and Figures 2 and 3 together with those for each of the other component transporters at the plasma membrane and tonoplast. A full description of each simulation and its outputs is unnecessary, and here we address only the most notable and intriguing of the results.

Figure 1, B and C, highlight both the sensitivity of simulations to a subset of transporters, primarily at the plasma membrane, and an asymmetry in efficacy

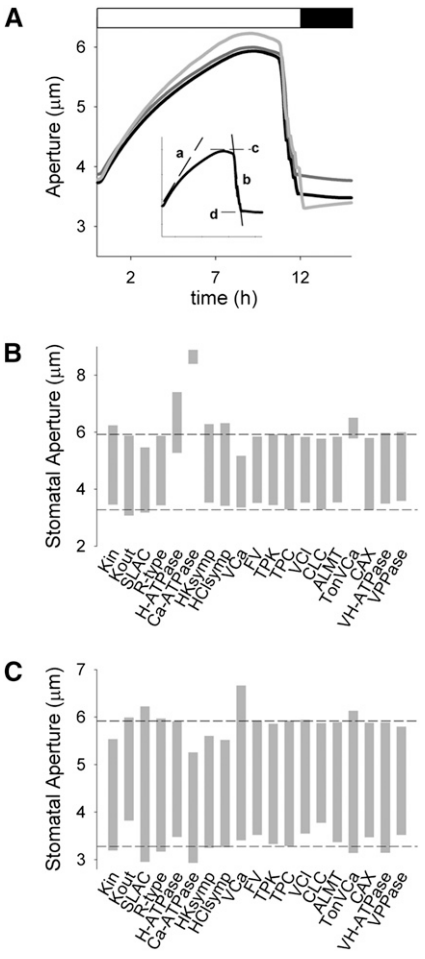

Figure 1. Selectively manipulating transporter population identifies a subset of transport activities that strongly influence stomatal dynamics. A, Aperture dynamics, in overlaid sections of 24-h cycles, of stomatal opening and closing simulated under control (black line) conditions and with the population of Kout (dark gray line) and anion channels (SLAC; light gray line) reduced by 50%. Analysis parameters of initial rates of opening (a) and closing (b) and maximum (c) and minimum (d) apertures as indicated. As previously described (Chen et al., 2012; Wang et al., 2012), light was used as a driver for Suc and malic acid synthesis, and for the ion-transporting ATPases at both membranes, and employed a $K_{1/2}$ for light intensity. The light cycle was driven through a sawtooth rise and fall over 12 h followed by 12 h of dark. Only part of the 12-h-dark period is shown, as indicated above with the white and black bars showing the transition times between light and dark. B and C, Dynamic range of apertures on elevating by 2-fold (B) and reducing to 50% (C) the population of each transporter. Horizontal lines indicate the dynamic range of the control simulation for comparison. Transporters at the plasma membrane are as follows: HClsymp, H^+-Cl^- symport; HKsymp, H^+-K^+ symport; R-type, R-type anion channel; SLAC, SLAC1-type anion channel; VCa, voltage-gated (inward-rectifying) Ca^{2+} channel. Transporters at the tonoplast are as follows: ALMT, voltage-gated ALMT-type (malate-permeable) anion channel; CAX, Ca^{2+}-H^+ antiporter; CLC, CLC-type H^+-Cl^- antiporter; FV, FV-type K^+ channel; TonVCa, voltage- and Ca^{2+}-gated Ca^{2+} channel; TPC, TPC1-type cation channel; TPK, TPK1-type K^+ channel; VCl, voltage-gated (inward-rectifying) Cl^- channel; VH-ATPase, V-type H^+-ATPase; VPPase, H^+-PPase. The properties and functions of each of these transporters are summarized in Hills et al. (2012).

between 0.5- and 2-fold changes in transporter populations. It also underscores the counterintuitive effects of manipulating many of these transporters. For example, the inward-rectifying K^+ channel (Kin), characterized by KAT1 in Arabidopsis (Nakamura et al., 1995), and the H^+-K^+ symporter (Rodriguez-Navarro et al., 1986; Blatt and Slayman, 1987; Maathuis and Sanders, 1994) serve as the two pathways for K^+ uptake. Increasing the densities of either of these transporters elevated the aperture maximum without effect on the minimum (Fig. 1B); however, reducing their densities suppressed both the maximum and minimum aperture values (Fig. 1C). An equally unexpected but inverted pattern was evident for Kout. By contrast, elevating the SLAC density reduced the aperture minimum and maximum, but reducing SLAC density led to an expanded dynamic range with a higher aperture maximum and, counterintuitively, a lower minimum. This asymmetry could be traced to the predicted dynamics in cytosolic-free $[Ca^{2+}]$ ($[Ca^{2+}]_i$), which is subject to membrane voltage (Grabov and Blatt, 1998; Sokolovski and Blatt, 2007) and feeds back on plasma membrane anion channel activities (Chen et al., 2012; Wang et al., 2012). In support of this conclusion, we note the parallel in asymmetry of manipulating transport affecting $[Ca^{2+}]_i$. For example, increasing the density of the Ca^{2+}-ATPase strongly elevated stomatal apertures, both the minimum and maximum; reducing the pump density reduced both the minimum and maximum, albeit with little effect on the dynamic range. Conversely, increasing the density of the hyperpolarization-activated Ca^{2+} channels (VCa) at the plasma membrane (Hamilton et al., 2000) suppressed the aperture maximum and dynamic range, whereas reducing Ca^{2+} channel density had the opposite effect. These characteristics are wholly consistent with the roles of these transporters in facilitating $[Ca^{2+}]_i$ elevation (low Ca^{2+}-ATPase, high Ca^{2+} channel densities) or its suppression (high Ca^{2+}-ATPase, low Ca^{2+} channel densities; McAinsh and Pittman, 2009; Pittman, 2011).

One fundamental prediction of OnGuard models, still to be demonstrated experimentally, is the existence of the endomembrane (vacuolar) Ca^{2+} channel, TonVCa (Chen et al., 2012; Hills et al., 2012). Essential features of this channel are its activation by $[Ca^{2+}]_i$ at submicromolar free concentrations and its inactivation at micromolar $[Ca^{2+}]_i$, analogous to the inositol-trisphosphate receptor channels in animals (Bezprozvanny et al., 1991; Hills et al., 2012). These characteristics give rise to prolonged oscillations in $[Ca^{2+}]_i$ that are thought to be essential in driving K^+ and Cl^- efflux for rapid stomatal closure (Grabov and Blatt, 1998; Blatt, 2000b; McAinsh and Pittman, 2009; Chen et al., 2012; Blatt et al., 2013). The counterintuitive effect of increasing TonVCa on aperture can be ascribed directly to the loss in these oscillations, arising from a reduction in the time-averaged total $[Ca^{2+}]$ from roughly 24 mM to 13 mM and a corresponding reduction in Ca^{2+} release. By contrast, decreasing the TonVCa population increased Ca^{2+} accumulation in the vacuole and the dynamic range of apertures. In

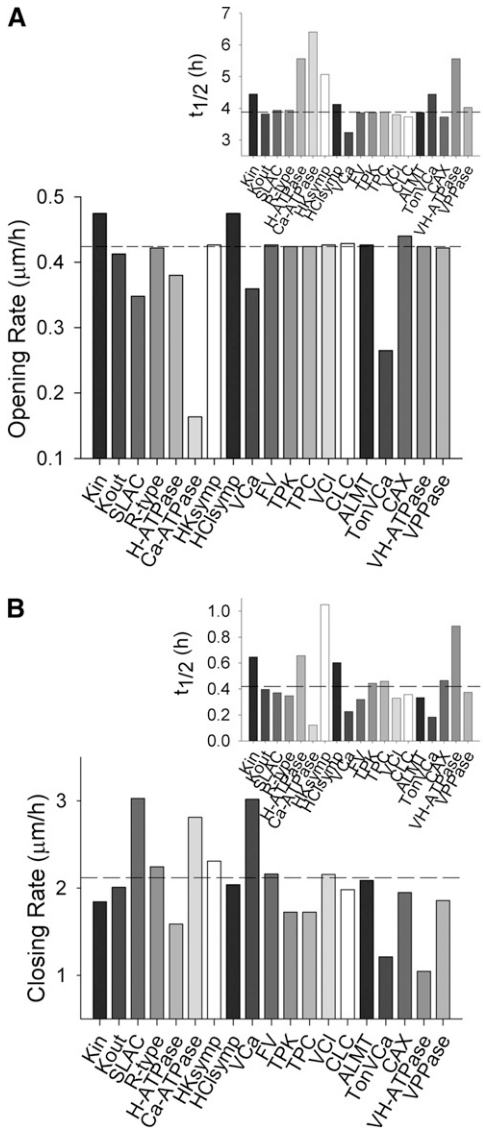

Figure 2. Selectively elevating transporter populations by 2-fold in simulations yields a subset of transport activities that affect the initial kinetics and the halftimes for response, but invariably affect both stomatal opening and closing. Transporter types are described in the legend to Figure 1. A, Initial rates of stomatal opening for elevation of each transporter population. The inset shows halftimes for opening. Horizontal lines in each case indicate the opening rate and halftime for the control simulation. B, Initial rates of stomatal closing for elevation of each transporter population. The inset shows halftimes for closing. Horizontal lines in each case indicate the closing rate and halftime for the control simulation.

short, manipulations affecting $[Ca^{2+}]_i$ are predicted to have the most profound effects on aperture, again in a seemingly counterintuitive manner. We note that Conn et al. (2011) reported an opposing effect associated with the Arabidopsis *cax1/cax3* double mutant lacking two of the dominant Ca^{2+}/H^+ exchangers that normally serve to sequester Ca^{2+} in endomembrane compartments. This mutant reduced Ca^{2+} accumulation in the leaf epidermis, the bulk of this in epidermal cells, and impaired stomatal dynamics and gas exchange. Their interpretation centered on elevated apoplastic $[Ca^{2+}]$, which is known to reduce stomatal apertures (de Silva et al., 1996; Webb et al., 2001). A direct comparison is complicated by a lack of data on the Ca^{2+} contents of the guard cells, and

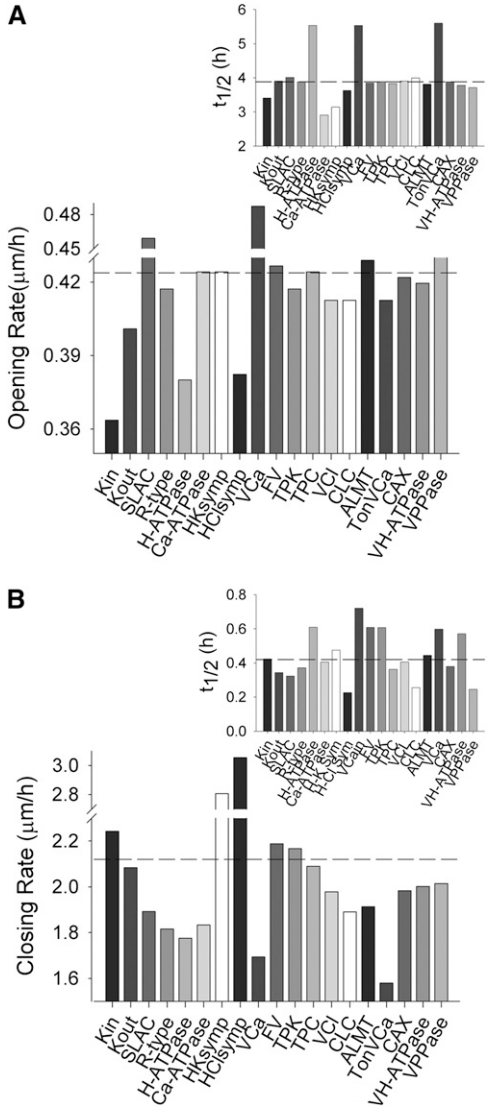

Figure 3. Selectively reducing transporter populations by 50% in simulations yields a subset of transport activities that affect the initial kinetics and the halftimes for response, but invariably affect both stomatal opening and closing. Transporter types are described in the legend to Figure 1. A, Initial rates of stomatal opening for elevation of each transporter population. The inset shows halftimes for opening. Horizontal lines in each case indicate the opening rate and halftime for the control simulation. B, Initial rates of stomatal closing for elevation of each transporter population. The inset shows halftimes for closing. Horizontal lines in each case indicate the closing rate and halftime for the control simulation.

by the fixed apoplastic $[Ca^{2+}]$ in our simulations. Nonetheless, the much reduced dynamic range in simulated apertures is consistent with the experimental findings.

In simulations with the H^+-ATPase, a 2-fold increase in population at the plasma membrane displaced the dynamic range of apertures to higher values, whereas decreasing the number of pumps to 50% of the control was marginal in effect. Here the asymmetry is the direct consequence of the nonlinearity in pump capacity (Blatt, 1987, 1988) and its parallel to that anticipated for charge balance through H^+-coupled transport (Sanders et al., 1985; Blatt and Slayman, 1987; Blatt and Clint, 1989; Maathuis and Sanders, 1994; Hills et al., 2012) and the inward-rectifying K^+ channels. Among others, the rise in aperture with H^+-ATPase activity is consistent with the known effects of locking the H^+-ATPase in an active state, either with the fungal toxin fusicoccin or in the *ost2* mutant (MacRobbie, 1988; Fuglsang et al., 1999; Merlot et al., 2007).

A complementary pattern was evident in the predicted rates for stomatal opening and closing. Figures 2 and 3 show the predicted rates for 2- and 0.5-fold changes in the numbers of each transporter, and insets within each figure summarize the halftimes for opening and closing. Again, the consequences of any one manipulation are generally evident in both opening and closing rates, often in counterintuitive ways that connect through changes in cytosolic pH and $[Ca^{2+}]_i$. For example, elevating the H^+-ATPase population led to decreases in both initial opening and closing rates and substantial increases in the halftimes for both processes (Fig. 2). These effects arose, in part, from a small elevation in cytosolic pH and the enhanced H^+ flux through coupled transport and malate metabolism, from plasma membrane hyperpolarization facilitating Ca^{2+} entry and $[Ca^{2+}]_i$ elevation, and from the reduced dynamic range of apertures. Even more surprising, modest reductions in opening and closing rates were also observed when the H^+-ATPase density was reduced (Fig. 3). In both cases, the effects can be ascribed to 0.1- to 0.2-pH unit shifts in cytosolic pH and, most important, in changes to $[Ca^{2+}]_i$ arising from the effects on the driving force for Ca^{2+} entry across the plasma membrane; in turn, these effects on cytosolic pH and $[Ca^{2+}]_i$ alternately affected K^+ flux through Kin and Kout and the balancing activities of the SLAC and R-type anion currents, much as documented by Wang et al. (2012).

It is noteworthy that several of the comparative predictions in Figure 2 are now confirmed. Coincident with the review of this article, independent experimental work was published by Wang et al. (2014), who demonstrated that a 3-fold overexpression of the AHA2 H^+-ATPase driven by a guard cell-specific promoter significantly enhanced stomatal conductance and opening in the light, and led to a small increase in carbon assimilation. Similar overexpression of two inward-rectifying K^+ channels, KAT1, which is normally expressed in guard cells, and AKT1, which is primarily

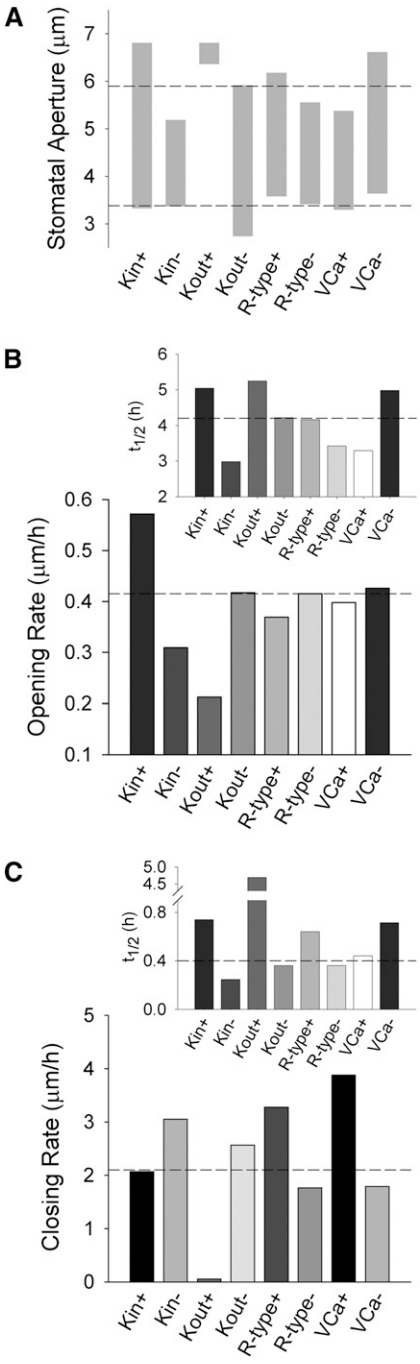

Figure 4. Altering the voltage ranges activating the major ion channels at the plasma membrane in simulations identifies the K^+ channels as targets for selectively enhancing stomatal opening and closing. Label signs (+ and −) refer to the midpoint voltage for gating ($V_{1/2}$) displacement from the control, either +18 mV or −18 mV. A, Dynamic range of apertures. Horizontal lines indicate the dynamic range of the control simulation for comparison. B, Initial rates of stomatal opening. The inset shows halftimes for opening. Horizontal lines in each case indicate the opening rate and halftime for the control simulation. C, Initial rates of stomatal closing. The inset shows halftimes for closing. Horizontal lines in each case indicate the closing rate and halftime for the control simulation.

found in roots, were without substantial effect on stomatal opening. They also found that overexpression of the H^+-ATPase reduced WUE, suggesting that this enhanced activity had other consequences for stomatal behavior, possibly in altering stomatal closure (Lawson and Blatt, 2014).

Manipulating Channel Gating

The midpoint voltage ($V_{1/2}$) for the gating of voltage-sensitive channels is subject to experimental modification (Tao et al., 2010; Pless et al., 2011), and mutations affecting $V_{1/2}$ are known for KAT1 (C. Lefoulon, C. Grefen, and M.R. Blatt, unpublished data). We found that stomatal aperture was equally sensitive in simulation to altering this parameter in the dominant ion channels at the plasma membrane. Uniquely for the K^+ channels, the effects were restricted primarily either to the opening or to the closing process. Most notable, manipulations of Kout to give an −18 mV shift in $V_{1/2}$ reduced the aperture minimum without substantial change to its maximum and accelerated closing (Fig. 4A). A corresponding +18 mV shift in $V_{1/2}$ for Kin affected primarily the aperture maximum, again without a proportional change in the minimum; similarly, it accelerated the initial opening rate by roughly 35% compared with the control without affecting closing. For manipulations of both Kin and Kout, the increases in halftimes related directly to the corresponding expansion in the dynamic ranges of apertures. These findings contrast with altering the gating characteristics of the SLAC current, which had compound effects on both opening and closing kinetics when assessed against changes in the dynamic ranges of apertures. Much the same conclusion was drawn from analysis of Ca^{2+} channel gating.

What defines the singular nature of Kin, and especially of Kout, to delimit the effects of manipulating their gating? Analysis of the underlying flux homeostasis for Kout, illustrated in Supplemental Figures S1 to S6, shows principally an absence of effect on either cytosolic pH or $[Ca^{2+}]_i$. Details are provided in the legends to Supplemental Figures S1 to S6, but can be summarized here. Kout normally activates together with anion currents by depolarization of the plasma membrane. Within the range of membrane voltages that activate Kout, changes to its activity have little impact on H^+ or Ca^{2+} flux across the plasma membrane, either through primary or secondary transport. Consequently, any changes in K^+ current are balanced primarily by alterations in anion efflux. So virtually all of the anticipated benefit of increasing the Kout population is offset by a change in free-running voltage as K^+ efflux adjusts with that of the anions. The voltage dependence of Kout and the anion channels are complementary, but for Kout this dependence is offset to voltages substantially positive of the anion channels, especially at millimolar K^+ concentrations and above. In these circumstances, displacing $V_{1/2}$ for Kout by −18 mV allows for K^+ and anion fluxes to balance at marginally more negative voltages, thereby yielding an enhanced capacity for the combined ion efflux. Otherwise, changes to Kout gating had no substantial consequences for the Ca^{2+} and voltage oscillations that are thought to drive solute efflux and stomatal closure.

In conclusion, we suggest that the gating characteristics of the dominant K^+ channels offer potential targets for genetic manipulation as a proof-of-principle in improving the WUE of plants. For reasons outlined above, it has been hypothesized that temporal mismatches between stomatal aperture and available light for photosynthesis significantly erode assimilation and WUE in fluctuating environments (Pearcy, 1990; Lawson et al., 2012; Lawson and Blatt, 2014). Thus, the challenge reduces to that of identifying, as candidates for manipulation, transporters that accelerate opening and closing, ideally both, without substantial constriction in the dynamic range of apertures. Achieving this goal has proven difficult, at least in simulation, because changes in transporter populations that were most effective in accelerating stomatal movements also led to counterintuitive and opposing effects on the complementary process, whether closing or opening. These findings lead us to discount simpler approaches that rely on altered expression of the wild-type transporters. It is important to recognize that these simulations are dissociated from feedback mechanisms affecting stomatal response through relative humidity, water supply, and pCO_2 within the leaf. In addition, the simulations do not account for the integrated sink strength of a crop (Baldocchi and Bowling, 2003), which may amplify the hysteresis in stomatal kinetics at leaf level by interactions between the multiple layers of a crop canopy. The consequences of manipulating channel gating as described here may well underestimate the impact on stomatal movements.

MATERIALS AND METHODS

OnGuard Modeling

The OnGuard software and model was driven through a diurnal 12-h-light/12-h-dark cycle as previously described (Chen et al., 2012) and all model outputs were derived from this cycle. Model parameters for *Vicia* (Hills et al., 2012) and Arabidopsis (*Arabidopsis thaliana*; Wang et al., 2012) were as described, the latter adjusted to reflect the physical dimensions of the Arabidopsis stomatal complex and transporter numbers scaled accordingly. Light sensitivity was assigned with a $K_{1/2}$ of 50 μmol m^{-2} s^{-1} solely to the plasma membrane H^+-ATPase and Ca^{2+}-ATPase, the vacuolar V-type H^+-ATPase, H^+-PPase and Ca^{2+}-ATPase, and to Suc (and, hence, malic acid) synthesis in accordance with experimental observation (Chen et al., 2012). All other model parameters were fixed, the properties of the individual transporters and buffering reactions thus responding only to changes in model variables arising from the kinetic features encoded in the model. The OnGuard software and the Arabidopsis model used in these simulations are available at http://www.psrg.org.uk.

Supplemental Data

The following materials are available in the online version of this article.

Supplemental Figure S1. Macroscopic outputs from the OnGuard model.

Supplemental Figure S2. K^+ contents and analysis of K^+ fluxes at the plasma membrane and tonoplast.

Supplemental Figure S3. Cytosolic and vacuolar pH, and H^+ fluxes across the plasma membrane and tonoplast.

Supplemental Figure S4. Chloride contents and analysis of Cl^- fluxes at the plasma membrane and tonoplast.

Supplemental Figure S5. Malic acid synthesis, total malate (Mal) contents, and analysis of $Mal2^-$ fluxes at the plasma membrane and tonoplast.

Supplemental Figure S6. Cytosolic and vacuolar [Ca^{2+}], cytosolic-free [Ca^{2+}], and analysis of Ca^{2+} fluxes across the plasma membrane and tonoplast.

Received December 2, 2013; accepted February 25, 2014; published March 4, 2014.

LITERATURE CITED

Baldocchi DD, Bowling DR (2003) Modelling the discrimination of $^{13}CO_2$ above and within a temperate broad-leaved forest canopy on hourly to seasonal time scales. Plant Cell Environ **26:** 231–244

Bezprozvanny I, Watras J, Ehrlich BE (1991) Bell-shaped calcium-response curves of Ins(1,4,5)P_3- and calcium-gated channels from endoplasmic reticulum of cerebellum. Nature **351:** 751–754

Blatt MR (1987) Electrical characteristics of stomatal guard cells: the contribution of ATP-dependent, "electrogenic" transport revealed by current-voltage and difference-current-voltage analysis. J Membr Biol **98:** 257–274

Blatt MR (1988) Mechanisms of fusicoccin action: a dominant role for secondary transport in a higher-plant cell. Planta **174:** 187–200

Blatt MR (2000a) $Ca^{(2+)}$ signalling and control of guard-cell volume in stomatal movements. Curr Opin Plant Biol **3:** 196–204

Blatt MR (2000b) Cellular signaling and volume control in stomatal movements in plants. Annu Rev Cell Dev Biol **16:** 221–241

Blatt MR, Clint GM (1989) Mechanisms of fusicoccin action: kinetic modification and inactivation of K(+) channels in guard cells. Planta **178:** 509–523

Blatt MR, Slayman CL (1987) Role of "active" potassium transport in the regulation of cytoplasmic pH by nonanimal cells. Proc Natl Acad Sci USA **84:** 2737–2741

Blatt MR, Wang Y, Leonhardt N, Hills A (2013) Exploring emergent properties in cellular homeostasis using OnGuard to model $K(^+)$ and other ion transport in guard cells. J Plant Physiol (in press)

Chen ZH, Hills A, Bätz U, Amtmann A, Lew VL, Blatt MR (2012) Systems dynamic modeling of the stomatal guard cell predicts emergent behaviors in transport, signaling, and volume control. Plant Physiol **159:** 1235–1251

Conn SJ, Gilliham M, Athman A, Schreiber AW, Baumann U, Moller I, Cheng NH, Stancombe MA, Hirschi KD, Webb AAR, et al (2011) Cell-specific vacuolar calcium storage mediated by *CAX1* regulates apoplastic calcium concentration, gas exchange, and plant productivity in *Arabidopsis*. Plant Cell **23:** 240–257

de Silva DLR, Honour SJ, Mansfield TA (1996) Estimations of apoplastic concentrations of K^+ and Ca^{2+} in the vicinity of stomatal guard cells. New Phytol **134:** 463–469

Eisenach C, Chen ZH, Grefen C, Blatt MR (2012) The trafficking protein SYP121 of *Arabidopsis* connects programmed stomatal closure and K^+ channel activity with vegetative growth. Plant J **69:** 241–251

Farquhar GD, von Caemmerer S, Berry JA, (2001) Models of photosynthesis. Plant Physiol **125:** 42–45

Fischer MJE, Paulussen JJC, Tollenaere JP, De Mol NJ, Janssen LHM (1998) Structure-activity relationships of astemizole derivatives for inhibition of store operated Ca^{2+} channels and exocytosis. Eur J Pharmacol **350:** 353–361

Fuglsang AT, Visconti S, Drumm K, Jahn T, Stensballe A, Mattei B, Jensen ON, Aducci P, Palmgren MG (1999) Binding of 14-3-3 protein to the plasma membrane H(+)-ATPase AHA2 involves the three C-terminal residues Tyr(946)-Thr-Val and requires phosphorylation of Thr(947). J Biol Chem **274:** 36774–36780

Grabov A, Blatt MR (1998) Membrane voltage initiates Ca^{2+} waves and potentiates Ca^{2+} increases with abscisic acid in stomatal guard cells. Proc Natl Acad Sci USA **95:** 4778–4783

Hamilton DWA, Hills A, Kohler B, Blatt MR (2000) Ca^{2+} channels at the plasma membrane of stomatal guard cells are activated by hyperpolarization and abscisic acid. Proc Natl Acad Sci USA **97:** 4967–4972

Hetherington AM, Woodward FI (2003) The role of stomata in sensing and driving environmental change. Nature **424:** 901–908

Hills A, Chen ZH, Amtmann A, Blatt MR, Lew VL (2012) OnGuard, a computational platform for quantitative kinetic modeling of guard cell physiology. Plant Physiol **159:** 1026–1042

Hosy E, Vavasseur A, Mouline K, Dreyer I, Gaymard F, Porée F, Boucherez J, Lebaudy A, Bouchez D, Very AA, et al (2003) The *Arabidopsis* outward K^+ channel GORK is involved in regulation of stomatal movements and plant transpiration. Proc Natl Acad Sci USA **100:** 5549–5554

Lawson T, Blatt MR (February 27, 2014) Size, speed and responsiveness of stomata impact on photosynthesis and water use efficiency. Plant Physiol

Lawson T, Kramer DM, Raines CA (2012) Improving yield by exploiting mechanisms underlying natural variation of photosynthesis. Curr Opin Biotechnol **23:** 215–220

Lawson T, von Caemmerer S, Baroli I (2011) Photosynthesis and stomatal behaviour. Prog Bot **72:** 265–304

Maathuis FJ, Sanders D (1994) Mechanism of high-affinity potassium uptake in roots of *Arabidopsis thaliana.* Proc Natl Acad Sci USA **91:** 9272–9276

MacRobbie EAC (1988) Stomatal guard cells. *In* **Baker DA, Hall JL**, eds, Solute Transport in Plant Cells and Tissues, Ed 1. Longman Press, Harlow, UK, pp 453–497

Masle J, Gilmore SR, Farquhar GD (2005) The ERECTA gene regulates plant transpiration efficiency in *Arabidopsis.* Nature **436:** 866–870

McAinsh MR, Pittman JK (2009) Shaping the calcium signature. New Phytol **181:** 275–294

Merlot S, Leonhardt N, Fenzi F, Valon C, Costa M, Piette L, Vavasseur A, Genty B, Boivin K, Müller A, et al (2007) Constitutive activation of a plasma membrane $H(^+)$-ATPase prevents abscisic acid-mediated stomatal closure. EMBO J **26:** 3216–3226

Nakamura RL, McKendree WL Jr, Hirsch RE, Sedbrook JC, Gaber RF, Sussman MR (1995) Expression of an Arabidopsis potassium channel gene in guard cells. Plant Physiol **109:** 371–374

Negi J, Matsuda O, Nagasawa T, Oba Y, Takahashi H, Kawai-Yamada M, Uchimiya H, Hashimoto M, Iba K (2008) CO_2 regulator *SLAC1* and its homologues are essential for anion homeostasis in plant cells. Nature **452:** 483–486

Ni BR, Pallardy SG (1992) Stomatal and nonstomatal limitations to net photosynthesis in seedlings of woody angiosperms. Plant Physiol **99:** 1502–1508

Pearcy RW (1990) Sunflecks and photosynthesis in plant canopies. Ann Rev Plant Physiol Plant Mol Biol **41:** 421–453

Pittman JK (2011) Vacuolar $Ca^{(2+)}$ uptake. Cell Calcium **50:** 139–146

Pless SA, Galpin JD, Niciforovic AP, Ahern CA (2011) Contributions of counter-charge in a potassium channel voltage-sensor domain. Nat Chem Biol **7:** 617–623

Rebetzke GJ, Condon AG, Richards RA, Farquhar GD (2002) Selection for reduced carbon isotope discrimination increases aerial biomass and grain yield of rainfed bread wheat. Crop Sci **42:** 739–745

Rodriguez-Navarro A, Blatt MR, Slayman CL (1986) A potassium-proton symport in *Neurospora crassa.* J Gen Physiol **87:** 649–674

Roelfsema MR, Hedrich R (2010) Making sense out of Ca(2+) signals: their role in regulating stomatal movements. Plant Cell Environ **33:** 305–321

Sanders D, Smith FA, Walker NA (1985) Proton/chloride cotransport in Chara: mechanism of enhanced influx after rapid external acidification. Planta **163:** 411–418

Schimel DS, House JI, Hibbard KA, Bousquet P, Ciais P, Peylin P, Braswell BH, Apps MJ, Baker D, Bondeau A, et al (2001) Recent patterns and mechanisms of carbon exchange by terrestrial ecosystems. Nature **414:** 169–172

Shimazaki KI, Doi M, Assmann SM, Kinoshita T (2007) Light regulation of stomatal movement. Annu Rev Plant Biol **58:** 219–247

Sokolovski S, Blatt MR (2007) Nitric oxide and plant ion channel control. *In* **Lamattina L, Polacco JC**, eds, Nitric Oxide in Plant Growth, Development and Stress Physiology, Ed 1. Springer, Berlin, pp 153–172

Tao X, Lee A, Limapichat W, Dougherty DA, MacKinnon R (2010) A gating charge transfer center in voltage sensors. Science **328:** 67–73

United Nations Educational, Scientific and Cultural Organization (2009) Water in a Changing World–UN World Water Development Report 3. United Nations Educational, Scientific and Cultural Organization, New York

Vico G, Manzoni S, Palmroth S, Katul G (2011) Effects of stomatal delays on the economics of leaf gas exchange under intermittent light regimes. New Phytol **192:** 640–652

Wang Y, Noguchi K, Ono N, Inoue S, Terashima I, Kinoshita T (2014) Overexpression of plasma membrane H^+-ATPase in guard cells promotes light-induced stomatal opening and enhances plant growth. Proc Natl Acad Sci USA **111:** 533–538 (in press)

Wang Y, Papanatsiou M, Eisenach C, Karnik R, Williams M, Hills A, Lew VL, Blatt MR (2012) Systems dynamic modeling of a guard cell Cl-channel mutant uncovers an emergent homeostatic network regulating stomatal transpiration. Plant Physiol **160:** 1956–1967

Webb AAR, Larman MG, Montgomery LT, Taylor JE, Hetherington AM (2001) The role of calcium in ABA-induced gene expression and stomatal movements. Plant J **26:** 351–362

Willmer C, Fricker MD (1996) Stomata, Vol **2**. Chapman and Hall, London

Supplemental Material for

Systems analysis of guard cell membrane transport for enhanced stomatal dynamics and water use efficiency

Yizhou Wang, Adrian Hills and Michael R. Blatt

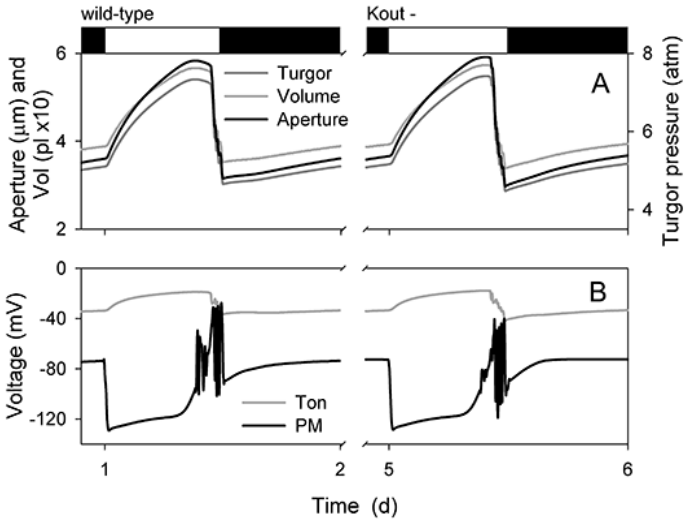

Fig. S1. Macrosocpic ouputs from the OnGuard model. Outputs resolved over a standard diurnal cycle (12 h light:12 h dark, indicated by bars above) with 10 mM KCl, 1 mM $CaCl_2$ and pH 6.5 outside (Chen et al. 2012). Representative diurnal cycles are shown for the wild-type (control, *left*) and Kout- manipulation (*right*), equivalent to a -18 mV shift in the mid-point voltage for GORK channel gating in Arabidopsis. For the results in this and the subsequent figures, the simulation was initiated with wild-type parameters (Wang et al. 2012) and the Kout- component current manipulated at the start of day 3, yielding a new stable cycle from day 4 onwards. A summary analysis is provided with each of the subsequent figures; further details will be found in Chen, et al. (2012). Shown are (A) stomatal aperture, turgor pressure and total guard cell volume, and (B) plasma membrane and tonoplast voltages. Stomatal apertures varied over a physiological range between roughly 3 µm and 6 µm in the wild-type and were parallelled by physiologically sensible changes in guard cell volume and turgor. Following stomatal closure at the end of the day, the model generated a small and gradual rise in aperture and the associated outputs that anticipated the start of the next day, much as has been observed in vivo (Gorton et al. 1993; Meidner and Willmer 1993). The start of the day was associated with hyperpolarisation of the plasma membrane to voltages near -130 mV and the dark period was marked by depolarisation of the plasma membrane to voltages near the equilibrium voltage for K^+, consistent with the diurnal cycle in energetic outputs of the ATP-driven pumps (Raschke 1979; Spanswick 1981; Blatt 1987; McClure et al. 1989; Blatt and Clint 1989; Clint and Blatt 1989; Kinoshita et al. 1995). Voltage oscillations at the end of the daylight period are detailed by Chen, et al. (2012) and mark periods of substantial K^+ and anion efflux that drive stomatal closure. These oscillations arise from coordinated oscillations in elevated $[Ca^{2+}]_i$ and enhanced K^+ and anion channel activity (see Supplemental Figs. S2, S4 and S6).

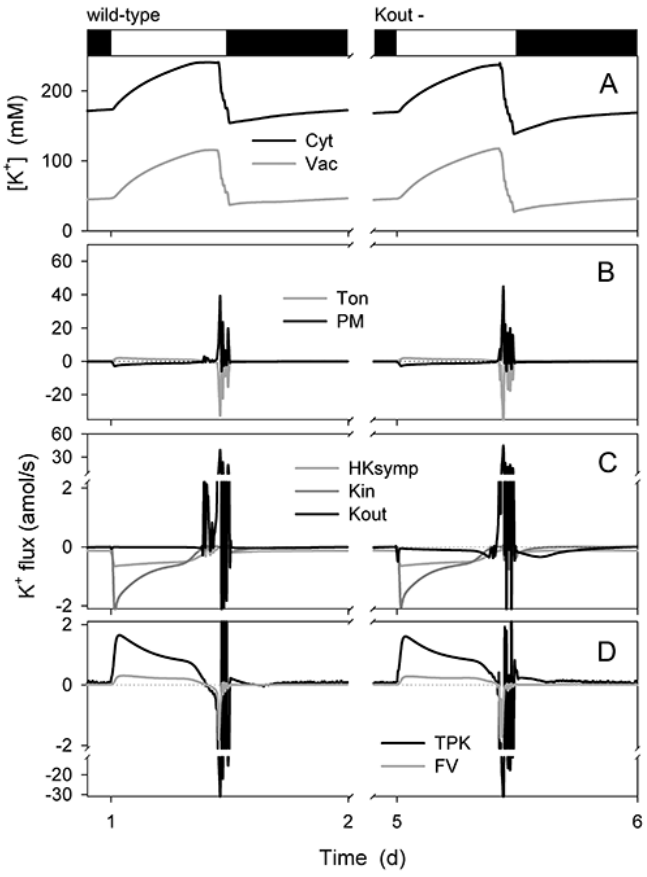

Fig. S2. K^+ contents and analysis of K^+ fluxes at the plasma membrane (PM) and tonoplast (Ton). Outputs resolved over a standard diurnal cycle (12 h light:12 h dark, indicated by bars above) (Chen et al. 2012) for the wild-type (control, *left*) and Kout- manipulation (*right*) as described in Supplemental Fig. S1. Shown are (A) cytosolic and vacuolar [K^+], (B) the net K^+ flux across the plasma membrane and tonoplast, (C) the K^+ flux through the K^+-permeable transporters at the plasma membrane, comprising the two K^+ channels and the H^+-K^+ symporter, and (D) the K^+ flux through the K^+ permeable transporters at the tonoplast, comprising the TPK and FV channels. K^+ flux through the TPC channel accounted for less than one percent of either of the other channel fluxes, and has therefore been omitted for purposes of clarity. Positive flux is defined as movement of the ionic species (not the charge) out of the cytosol, either across the plasma membrane or the tonoplast. Note that the bulk of K^+ entering across the plasma membrane is shunted across the tonoplast to the vacuole during the day and this pattern reversed in the first hours of dark, as expected from experimental observation (Hills et al. 2012; Chen et al. 2012). At the plasma membrane (C), K^+ influx was dominated by $I_{K,in}$ in the first half of the day, and roughly matched by flux through the H^+-K^+ symport in the second half of the day. Closure was marked by the predominance of K^+ efflux through Kout which relaxed to a near-zero value during the night. These simulations show a minor influx through Kout at the end of the daylight period when manipulated to open at the more negative voltages. This additional influx accounts in part for the small elevation in aperture maximum (Fig. S1), but has no substantial effect otherwise. Modifying Kout facilitates oscillations and K^+ efflux at the end of the daylight period and leads to a small decrease in the minimum aperture and acceleration of initial reopening in the dark.

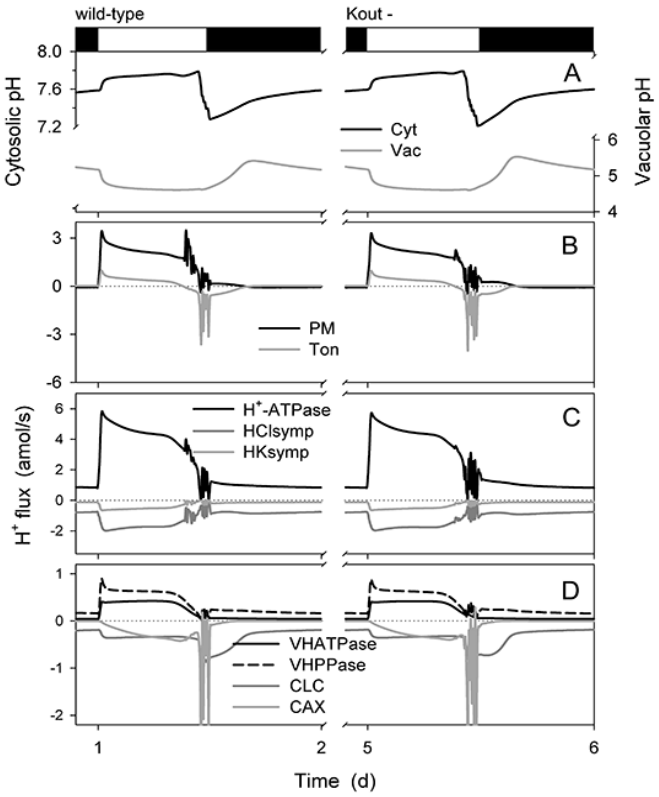

Fig. S3.Cytosolic and vacuolar pH, and H^+ fluxes across the plasma membrane and tonoplast. Outputs resolved over a standard diurnal cycle (12 h light:12 h dark, indicated by bars above) (Chen et al. 2012) for the wild-type (control, *left*) and Kout- manipulation (*right*) as described in Supplemental Fig. S1. Shown are (A) cytosolic and vacuolar pH, (B) the net H^+ flux across the plasma membrane and tonoplast, (C) the H^+ flux through the H^+-permeable transporters at the plasma membrane, comprising the H^+-ATPase, and the H^+-K^+ and H^+-Cl^- symporters, and (D) the H^+ flux through the H^+ permeable transporters at the tonoplast, comprising the VH^+-ATPase, VH^+-PPase, the CLC H^+-Cl^- antiporter and the CAX H^+-Ca^{2+} antiporter. Positive flux is defined as movement of the ionic species (not the charge) out of the cytosol, either across the plasma membrane or the tonoplast. The bulk of H^+ production associated with daytime Mal synthesis (Supplemental Fig. S5) is exported via the plasma membrane H^+-ATPase, with roughly 20% transported to the vacuole (B-D). In the vacuole, Mal comprises the major pH buffer and its accumulation is associated with acidification of the vacuolar contents (Van Kirk and Raschke 1978; Outlaw 1990; Talbott and Zeiger 1993; Willmer and Fricker 1996). Diurnal changes in vacuolar pH in the model resulted primarily from Mal transport and charge balance with H^+ (Supplemental Fig. S5). The organic acid is thought to be transported as the fully deprotonated (Mal^{2-}) form – with the ALMT channel as the primary pathway for tonoplast Mal^{2-} flux [reviewed by Hills, et al. (Hills et al. 2012)] – implying charge balance via the tonoplast VH^+-ATPase and H^+-PPase (Rea and Poole 1993; Martinoia et al. 2007). Minor effects of the modification of Kout gating are visible in depression of cytosolic pH at the end of the daylight period and arise from a small change in H^+ fluxes at this time, mainly through the H^+-ATPase and CLC H^+-Cl^- antiporter.

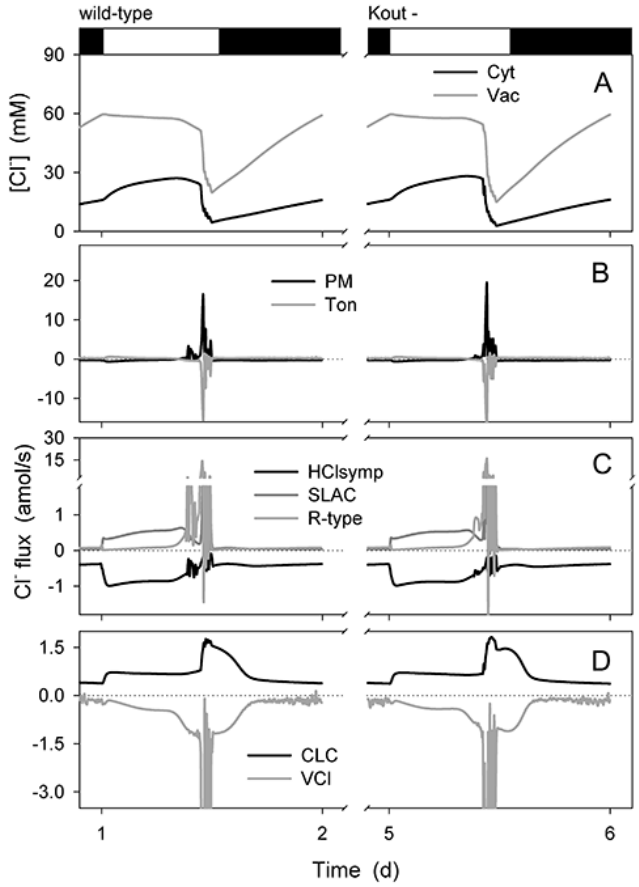

Fig. S4. Chloride contents and analysis of Cl^- fluxes at the plasma membrane and tonoplast. Outputs resolved over a standard diurnal cycle (12 h light:12 h dark, indicated by bars above) (Chen et al. 2012) for the wild-type (control, *left*) and Kout- manipulation (*right*) as described in Supplemental Fig. S1. Shown are (A) total cytosolic and vacuolar [Cl^-], (B) the net flux of Cl^- across the plasma membrane and tonoplast, (C) the flux of Cl^- through the Cl^--permeable transporters at the plasma membrane, comprising the SLAC and R-type anion channels and H^+-Cl^- symporter, and (D) the flux of Cl^- through the Cl^--permeable transporters at the tonoplast, comprising the VCl channel and CLC H^+-Cl^- antiporter. Positive flux is defined as movement of the ionic species (not the charge) out of the cytosol, either across the plasma membrane or the tonoplast. Note the expanded scales in (C) and (D). Both wild-type and Kout- modifications yield cytosolic and vacuolar Cl^- concentrations that exhibit complex, biphasic responses to the diurnal cycle, in effect leading to an exchange of Cl^- for Mal accumulated in the daytime and vice versa at night (compare Supplemental Fig. S5) (Raschke and Schnabl 1978; Talbott and Zeiger 1993; Talbott and Zeiger 1996). Stomatal opening was accompanied by a net efflux of Cl^- from the vacuole to the cytosol and, later in the daylight period from the cytosol to the apoplast. Closure was marked by much larger fluxes of Cl^- from the vacuole to the cytosol and export across the plasma membrane; this pattern reversed after the first 1-2 h of dark. The rise in cytosolic Cl^- concentration during the first hours of the day arose from the rapid Cl^- influx across the tonoplast and a slower rise in the rate of Cl^- export across the plasma membrane. Modifying Kout gating leads only to an enhanced efflux at the plasma membrane and, at the tonoplast, through the CLC antiporter at the end of the daylight period.

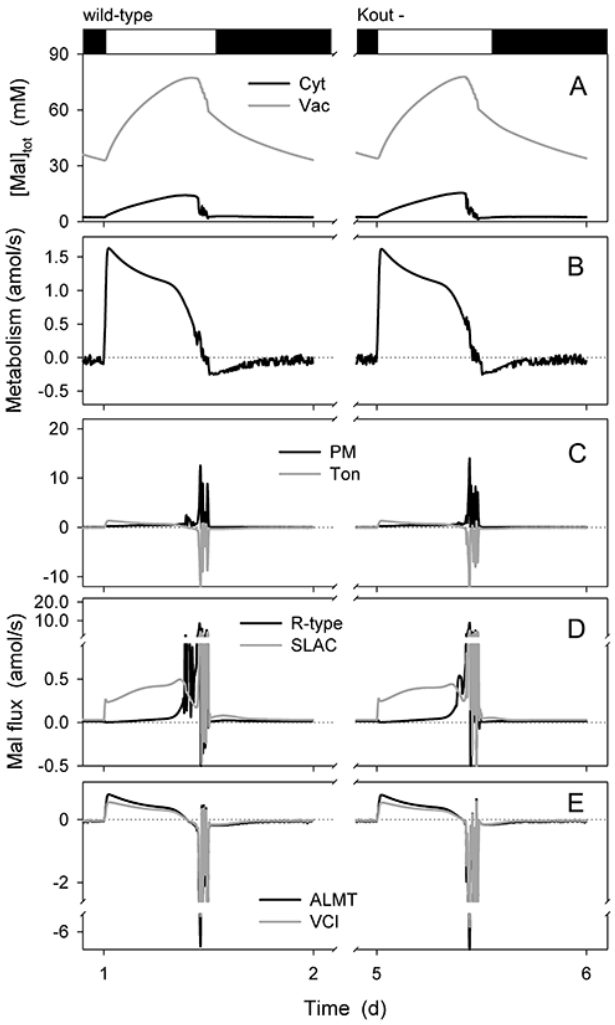

Fig. S5. Malic acid synthesis, total malate (Mal) contents and analysis of Mal^{2-} fluxes at the plasma membrane and tonoplast. Outputs resolved over a standard diurnal cycle (12 h light:12 h dark, indicated by bars above) (Chen et al. 2012) for the wild-type (control, *left*) and Kout- manipulation (*right*) as described in Supplemental Fig. S1. Shown are (A) total cytosolic and vacuolar [Mal], (B) the rates of Mal synthesis and metabolism, (C) the net flux of Mal^{2-} across the plasma membrane and tonoplast, (D) the Mal^{2-} flux through the Mal^{2-}-permeable transporters at the plasma membrane, comprising the SLAC and R-type anion channels, and (E) the Mal^{2-} flux through the Mal^{2-} permeable transporters at the tonoplast, comprising the ALMT and VCl channels. Positive flux is defined as movement of the ionic species (not the charge) out of the cytosol, either across the plasma membrane or the tonoplast. These simulations, show no substantial effect modifying Kout gating. In both cases, the bulk of Mal production was diverted by transport of Mal^{2-} across the tonoplast, leading to a rise in total vacuolar Mal from 30 mM at the end of the night to near 90 mM before declining at the end of the daylight period; Mal in the cytosol rose from approximately 1 mM to values near 15 mM, much as estimated from experimental data and summarised previously (Hills et al. 2012). Mal efflux at the plasma membrane is predicted to be mediated largely by the SLAC-type anion channel during daylight with the added contribution of flux through the R-type anion channel during stomatal closure.

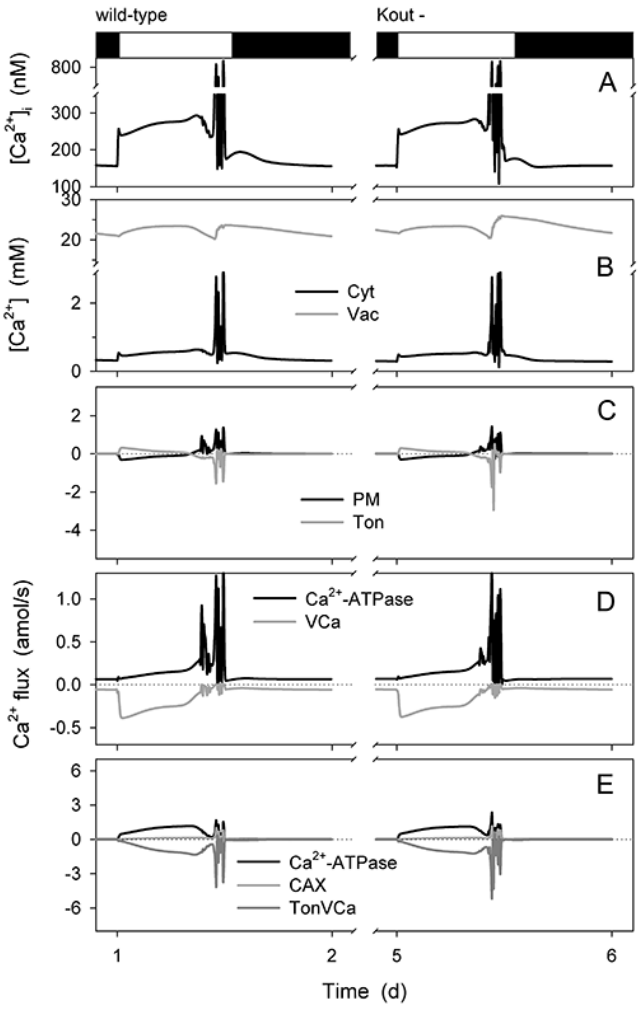

Fig. S6. Cytosolic and vacuolar [Ca^{2+}], cytosolic-free [Ca^{2+}] ([Ca^{2+}]$_i$), and analysis of Ca^{2+} fluxes across the plasma membrane and tonoplast. Outputs resolved over a standard diurnal cycle (12 h light:12 h dark, indicated by bars above) (Chen et al. 2012) for the wild-type (control, *left*) and Kout-manipulation (*right*) as described in Supplemental Fig. S1. Shown are (A) the cytosolic-free [Ca^{2+}], (B) the total [Ca^{2+}], (C) the net flux of Ca^{2+} across the plasma membrane and tonoplast, (D) the Ca^{2+} flux through the Ca^{2+}-permeable transporters at the plasma membrane, comprising the hyperpolarisation-activated Ca^{2+} channel VCa and the Ca^{2+}-ATPase, and (E) the flux of Ca^{2+} through the Ca^{2+}-permeable transporters at the tonoplast, comprising the Ca^{2+}-ATPase, the CAX H^+-Ca^{2+} antiporter, and the TonVCa Ca^{2+} channel. Flux through the TPC channel accounts for less than two percent of the total Ca^{2+} flux across the tonoplast and has therefore been omitted for purposes of clarity. Positive flux is defined as movement of the ionic species (not the charge) out of the cytosol, either across the plasma membrane or the tonoplast. Both in wild-type and modified Kout simulations[Ca^{2+}]$_i$ is predicted to rise from a resting value near 160 nM in the dark to a mean daylight value near 260 nM (A). Stomatal closure is accompanied by a series of voltage (Supplemental Fig. S1) and [Ca^{2+}]$_i$ oscillations that drive K^+ and anion efflux during closure (Gilroy et al. 1991; Thiel et al. 1992; Irving et al. 1992; McAinsh et al. 1992; Blatt and Armstrong 1993; Gradmann et al. 1993; Grabov and Blatt 1998; Staxen et al. 1999). Further details will be found in Chen, et al. (Chen et al. 2012). Vacuolar Ca^{2+} circulation dominates over transport at the plasma membrane by at least one order of magnitude (Sanders et al. 2002; Blatt et al. 2007; McAinsh and Pittman 2009) and is essential to potentiating [Ca^{2+}]$_i$ signals (Gilroy et al. 1991; McAinsh et al. 1991; Grabov and Blatt 1997; Grabov and Blatt 1998; Grabov and Blatt 1999; Garcia-Mata et al. 2003). Again, these results show no substantial difference between the two simulations.

References:

1. Blatt MR (1987) Electrical characteristics of stomatal guard cells: the ionic basis of the membrane potential and the consequence of potassium chloride leakage from microelectrodes. Planta 170: 272-287

2. Blatt MR, Armstrong F (1993) K^+ channels of stomatal guard cells: abscisic acid-evoked control of the outward rectifier mediated by cytoplasmic pH. Planta 191: 330-341

3. Blatt MR, Clint GM (1989) Mechanisms of fusicoccin action kinetic modification and inactivation of potassium channels in guard cells. Planta 178: 509-523

4. Blatt MR, Garcia-Mata C, Sokolovski S (2007) Membrane transport and Ca^{2+} oscillations in guard cells. In S Mancuso, S Shabala, eds, Rhythms in Plants, Ed 1. Springer, Berlin, pp 115-134

5. Chen ZH, Hills A, Baetz U, Amtmann A, Lew VL, Blatt MR (2012) Systems Dynamic Modeling of the Stomatal Guard Cell Predicts Emergent Behaviors in Transport, Signaling, and Volume Control. Plant Physiol 159: 1235-1251

6. Clint GM, Blatt MR (1989) Mechanisms of fusicoccin action: evidence for concerted modulations of secondary K^+ transport in a higher-plant cell. Planta 178: 495-508

7. Garcia-Mata C, Gay R, Sokolovski S, Hills A, Lamattina L, Blatt MR (2003) Nitric oxide regulates K^+ and Cl^- channels in guard cells through a subset of abscisic acid-evoked signaling pathways. Proc Natl Acad Sci USA 100: 11116-11121

8. Gilroy S, Fricker MD, Read ND, Trewavas AJ (1991) Role of calcium in signal transduction of Commelina guard cells. Plant Cell 3: 333-344

9. Gorton HL, Williams WE, Assmann SM (1993) Circadian rhythms in stomatal responsiveness to red and blue light. Plant Physiol 103: 399-406

10. Grabov A, Blatt MR (1997) Parallel control of the inward-rectifier K^+ channel by cytosolic-free Ca^{2+} and pH in *Vicia* guard cells. Planta 201: 84-95

11. Grabov A, Blatt MR (1998) Membrane voltage initiates Ca^{2+} waves and potentiates Ca^{2+} increases with abscisic acid in stomatal guard cells. Proc Natl Acad Sci USA 95: 4778-4783

12. Grabov A, Blatt MR (1999) A steep dependence of inward-rectifying potassium channels on cytosolic free calcium concentration increase evoked by hyperpolarization in guard cells. Plant Physiol 119: 277-287

13. Gradmann D, Blatt MR, Thiel G (1993) Electrocoupling of ion transporters in plants. J Membr Biol 136: 327-332

14. Hills A, Chen ZH, Amtmann A, Blatt MR, Lew VL (2012) OnGuard, a Computational Platform for Quantitative Kinetic Modeling of Guard Cell Physiology. Plant Physiol 159: 1026-1042

15. Irving HR, Gehring CA, Parish RW (1992) Changes in cytosolic pH and calcium of guard

cells precede stomatal movements. Proc Natl Acad Sci USA 89: 1790-1794

16. Kinoshita T, Nishimura M, Shimazaki KI (1995) Cytosolic concentration of Ca2+ regulates the plasma membrane H^+- ATPase in guard cells of fava bean. Plant Cell 7: 1333-1342

17. Martinoia E, Maeshima M, Neuhaus HE (2007) Vacuolar transporters and their essential role in plant metabolism. J Exp Bot 58: 83-102

18. McAinsh MR, Brownlee C, Hetherington AM (1991) Partial inhibition of ABA-induced stomatal closure by calcium- channel blockers. Proc R Soc Lond Ser B Biol Sci 243: 195-202

19. McAinsh MR, Brownlee C, Hetherington AM (1992) Visualizing changes in cytosolic-free Ca^{2+} during the response of stomatal guard cells to abscisic acid. Plant Cell 4: 1113-1122

20. McAinsh MR, Pittman JK (2009) Shaping the calcium signature. New Phytol 181: 275-294

21. McClure PR, Shaff JE, Spanswick RM, Kochian LV (1989) Response of the membrane potential of maize roots to nitrate Plant Physiol 89: S-45

22. Meidner H, Willmer CM (1993) Circadian rhythm of stomatal movements in epidermal strips. J Exp Bot 44: 1649-1652

23. Outlaw WHJ (1990) Kinetic properties of guard-cell phosphoenolpyruvate carboxylase. Biochem Physiol Pflanzen 186: 317-326

24. Raschke K (1979) Movements of stomata. In W Haupt, ME Feinleib, eds, Encyclopedia of Plant Physiology, N.S. Vol. 7, Ed 1. Springer, Berlin, pp 373-441

25. Raschke K, Schnabl H (1978) Availability of chloride affects balance between potassium chloride and potassium malate in guard cells of Vicia faba L. Plant Physiol 62: 84-87

26. Rea PA, Poole RJ (1993) Vacuolar H^+-translocating pyrophosphatase. Ann Rev Plant Physiol Mol Biol 44: 157-180

27. Sanders D, Pelloux J, Brownlee C, Harper JF (2002) Calcium at the crossroads of signaling. Plant Cell 14: S401-S417

28. Spanswick RM (1981) Electrogenic ion pumps. Ann Rev Plant Physiol Mol Biol 32: 267-281

29. Staxen I, Pical C, Montgomery LT, Gray JE, Hetherington AM, McAinsh MR (1999) Abscisic acid induces oscillations in guard-cell cytosolic free calcium that involve phosphoinositide-specific phospholipase C. Proc Natl Acad Sci USA 96: 1779-1784

30. Talbott LD, Zeiger E (1993) Sugar and organic acid accumulation in guard cells of *Vicia faba* in response to red and blue light. Plant Physiol 102: 1163-1169

31. Talbott LD, Zeiger E (1996) Central roles for potassium and sucrose in guard cell osmoregulation. Plant Physiol 111: 1051-1057

32. Thiel G, MacRobbie EAC, Blatt MR (1992) Membrane transport in stomatal guard cells: the importance of voltage control. J Membr Biol 126: 1-18

33. Van Kirk CA, Raschke K (1978) Presence of chloride reduces malate production in epidermis during stomatal opening. Plant Physiol 61: 361-364

34. Wang Y, Papanatsiou M, Eisenach C, Karnik R, Williams M, Hills A, Lew VL, Blatt MR (2012) Systems dynamic modelling of a guard cell Cl^- channel mutant uncovers an emergent homeostatic network regulating stomatal transpiration. Plant Physiol 160: 1956-1972

35. Willmer C, Fricker MD. Stomata. 1996. London, Chapman and Hall.